Journal of Hazardous Materials 213–214 (2012) 434–439

Contents lists available at SciVerse ScienceDirect

Journal of Hazardous Materials

journal homepage: www.elsevier.com/locate/jhazmat

The effect of hardness on the stability of citrate-stabilized gold nanoparticles and their uptake by *Daphnia magna*

Byung-Tae Lee, James F. Ranville*

Department of Chemistry and Geochemistry, Colorado School of Mines, Golden, CO 80401, USA

ARTICLE INFO

Article history:
Received 27 June 2011
Received in revised form 30 January 2012
Accepted 8 February 2012
Available online 16 February 2012

Keywords:
Nanoparticles
Aggregation
Fractal dimension
Daphnia
Uptake

ABSTRACT

The stability and uptake by *Daphnia magna* of citrate-stabilized gold nanoparticles (AuNPs) in three different hardness-adjusted synthetic waters were investigated. Negatively charged AuNPs were found to aggregate and settle in synthetic waters within 24 h. Sedimentation rates depended on initial particle concentrations of 0.02, 0.04, and 0.08 nM AuNPs. Hardness of the synthetic waters affected the aggregation of AuNPs and is explained by the compression of diffuse double layer of AuNPs due to the increasing ionic strength. The fractal dimension of AuNPs in the reaction-limited regime of synthetic waters averaged 2.228 ± 0.126 implying the rigid structures of aggregates driven by the collision of small particles with the growing aggregates. Four-day old *D. magna* accumulated more than 90% of AuNPs in 0.04 nM AuNP suspensions without any observed mortality. Exposure to pre-aggregated AuNP for 48 h in hard water did not show any significant difference in uptake, suggesting *D. magna* can also ingest settled AuNP aggregates. *D. magna* exposed to AuNPs shed their exoskeleton whereas the control did not generate any molts over 48 h. This implies that *D. magna* removed AuNPs on their exoskeleton by producing molts to decrease any adverse effects of adhered AuNPs.

1. Introduction

Nanomaterials are being used in a wide array of products, which leads to an increase in the potential for environmental risk. Numerous studies have reported that engineered nanoparticles (ENPs) cause toxic effects on cells by induction of reactive oxygen species [1] or by release of toxic metals [2,3]. Fewer investigations have looked for other modes of toxicity such as attachment of ENPs to biological surfaces, leading to physical impairment of organism behavior or health [4,5]. Polymer coatings are added to enhance ENP aqueous stability through both steric and electrostatic mechanisms [6]. These coatings may be inherently toxic or may facilitate the uptake of ENPs by the organism and therefore play an important role in the potential for organism exposure to ENP because of their control on aggregation and sedimentation, and/or dissolution [2]. There are several different exposure pathways of nanomaterials that result in release to water, soil, and air. When the nanoparticles are introduced into environmental media, they move through these pathways and are accumulated in various destinations such as wastewater, soils, landfills, among others [7,8]. Traveling through these pathways, the nanoparticles can encounter changes in their chemical environment, potentially leading to the alteration of their surface properties. Studies have shown that suspension stability of nanoparticles has been significantly affected by pH [9,10] and ionic strength [10–12], and that nanoparticle stability is controlled by the compression of the diffuse double layer which leads to aggregation [10,11]. Therefore, emphasis must be placed on the study of surface properties, which directly influence ENP fate and transport in the environmental media in order to better understand ENP environmental threats or risks.

Gold nanoparticles (AuNPs) are very useful as a "model particle" in examining ENP dynamics and bioaccumulation, as they are insoluble and are relatively non-toxic. They are also currently used in biomedical diagnosis and sensing [13,14], and are used in numerous electronic or chemical applications [15,16] as well. These wide uses of AuNPs can result in their exposure to the environment and supports the need to study biological uptake, stability, and their fate and transport in aquatic environments. One of the typical stabilizers for AuNPs is citrate, which may have a significant role in their transport through aqueous environments [17,18]. Few studies have dealt directly with AuNP environmental stability [11,19]. Humic substances interact with ENP surfaces and can play an important role in the aggregation of AuNPs [19]. However little is known about how humic substances may interact, modify, or even replace the initial surface stabilizers. Furthermore, most ENP stability studies have used aqueous phases with ionic strength adjusted by a single counterion, such as Ca^{2+}or Na^{+}, and have not used more environmentally relevant conditions such as hard, moderately hard, or soft water [10–12].

* Corresponding author. Tel.: +1 303 273 3004; fax: +1 303 273 3629.
E-mail address: jranvill@mines.edu (J.F. Ranville).

0304-3894/$ – see front matter © 2012 Elsevier B.V. All rights reserved.
doi:10.1016/j.jhazmat.2012.02.025

The freshwater crustacean *Daphnia magna* is a representative organism used in aquatic toxicity testing [20]. Due to their sensitivity to many hazardous substances, it has been widely used for toxicity assessments of nanoparticles in aquatic environments [5,21]. *D. magna* has reported to ingest a significant amount of various types of nanoparticles and retain them in their digestive track [5,22]. Furthermore, surface adsorption of nanoparticles onto the exterior of *D. magna* limit their biological activity and led to mortality [4,5]. Previous studies have focused on the toxicity of nanoparticles on *D. magna*, with limited information reported on the role of surface chemistry, which is important in NP uptake and accumulation.

The aim of the study was to further our understanding of ENP aquatic exposure by simultaneously examining the stability and biological uptake of AuNPs. We characterized the aggregation and sedimentation of citrate-stabilized AuNPs in three synthetic waters of varying hardness. Effects of particle concentration and hardness on aggregation of AuNPs were evaluated with respect to the aggregation rate constants, obtained by UV–vis spectroscopy, and fractal dimensions, obtained from determination of hydrodynamic size using dynamic light scattering. We hypothesized that differing hardnesses would result in different aggregation states and rates, which might affect the ingestion or surface adsorption of AuNPs by *D. magna*. AuNPs exposures were performed in the synthetic waters and the uptake by *D. magna* was assessed by ICP-AES. Furthermore, AuNPs were also pre-aggregated in hard water and then exposed to *D. magna* to more fully evaluate the effect of aggregation state on uptake.

2. Materials and methods

2.1. Preparation and characterization of citrate-stabilized gold nanoparticles.

Gold nanoparticles with an approximate diameter of 20 nm were synthesized using the modified Turkevich method [17]. Briefly, 30 mL of 0.25 mM $HAuCl_4$ solution was added to Erlenmeyer flasks and heated to 80 °C. Once a stable temperature was achieved, Au^{3+} solution was reduced by adding 1.5 mL of 1% sodium citrate solution. The solution was maintained at that temperature until the solution turned ruby red, indicating AuNP had formed. After cooling to room temperature, small portions were taken for UV–vis analysis (Model DU8000, Beckman Coulter). Hydrodynamic size was also determined by dynamic light scattering (Zetasizer nanoseries, Malvern Instrument) with a 633 nm laser source and a detection angle of 173°. Electrophoretic mobility was also measured using the same instrument and subsequently converted to zeta potential by the Smoluchowscki's approximation [23]. Transmission electron microscopy (TEM) images were obtained for determination of the size and shape of the AuNPs. Samples were prepared on a carbon coated copper grid and images were captured by TEM (JEOL, JEM-2010) operated at 200 kV.

2.2. Aggregation and sedimentation of AuNPs in synthetic waters

Before experiments, the AuNP suspensions were sonicated in a low-power bath for 10 min. Synthetic hard water was prepared using nanopure water and analytical grade chemicals (Supporting information Table S1) [20]. Aliquots of AuNP suspensions were then added to yield 0.02, 0.04, and 0.08 nM of AuNPs as particle concentration (1.3, 2.6, and 5.2 mg L^{-1} as total Au concentrations, respectively. AuNP concentrations are expressed with nM as particle concentration throughout the text.). In order to monitor the rate of sedimentation, samples were taken at the upper layer (1 cm) of the suspensions using a digital pipette at appropriate time intervals over 24 h. Hydrodynamic size was immediately measured by DLS (Brookhaven ZetaPlus™, Brookhaven Instruments) and UV–vis spectrum was collected. Samples were digested using *aqua regia* at 80 °C for 2 h and Au concentrations were then determined by ICP-AES (ICP-AES 5300DV, PerkinElmer). Moderately hard and soft synthetic waters were prepared by diluting a stock solution of synthetic hard water by a factor of 2 and 4 times respectively. Suspensions were prepared in these two waters at 0.04 nM AuNP and measured using the same procedures as were used in the hard water experiments.

2.3. D. magna exposure to AuNP suspensions

D. magna were cultured in the laboratory and fed algae and seaweed extract following EPA standard protocols [2]. Four-day old *D. magna* were used in the study. Forty *D. magna* were selected and rinsed with clean synthetic hard water and were placed in a 100 mL glass beaker containing 80 mL of test water. AuNP suspensions were briefly sonicated then sufficient volume was transferred to make a concentration of 0.04 nM of AuNP. AuNP suspensions were sampled and measured by UV–vis spectrophotometer over a period of 48 h. Hard and moderately hard synthetic waters were used for *D. magna* exposure experiments. To observe the effect of aggregates on *D. magna*, AuNP suspensions were added into synthetic hard water and left for 48 h to allow aggregation and sedimentation before the addition of *D. magna* into the suspensions. After 48 h of exposure to AuNP suspensions, all *D. magna* and their molts were collected separately and transferred into 15 mL tubes, after rinsing with DI water several times. Each sample was digested using *aqua regia* and analyzed by ICP-AES. Mass balance of Au throughout the study showed 102–117% recoveries for the sum of Au in molts, *D. magna*, and in suspension after 48 h exposure to AuNP suspensions. The average dry mass of 4-day old *D. magna* was 0.044 ± 0.023 mg.

3. Results and discussion

3.1. Characterization of synthesized AuNPs

The properties of the stock AuNPs suspensions are summarized in Table 1. UV–vis spectra of citrate-stabilized AuNPs showed a symmetrical single peak with maximum absorption at 521 nm (Supporting information Fig. S1). TEM showed that the as-prepared AuNPs were monodispersed (Supporting information Fig. S2). Analysis of TEM images showed that the average diameter was 17.0 ± 1.7 nm which was not in perfect agreement with the DLS measurement that gave the average hydrodynamic size of 21.6 ± 0.6 nm in *z*-average. The differences between two measurements may be due to the citrate layer of AuNPs and the diffuse double layers on the particle surface. The small standard deviations

Table 1
Characteristics of the citrate-stabilized AuNPs. TEM size represents the average diameter ± SD (n = 143), hydrodynamic size is the *z*-average measured by DLS (avg. ± SD, n = 3), the values of zeta potential are avg. ± SD (n = 3).

	TEM size (nm)	Hydrodynamic size (nm)	UV 1st peak position (nm)	Zeta potential (mV)			
				pH 4	pH 6	pH 8	pH 10
Citrate-AuNPs	17.0 ± 1.7	21.6 ± 0.6	521	−24.9 ± 6.5	−22.3 ± 6.9	−33.5 ± 7.1	−45.4 ± 4.1

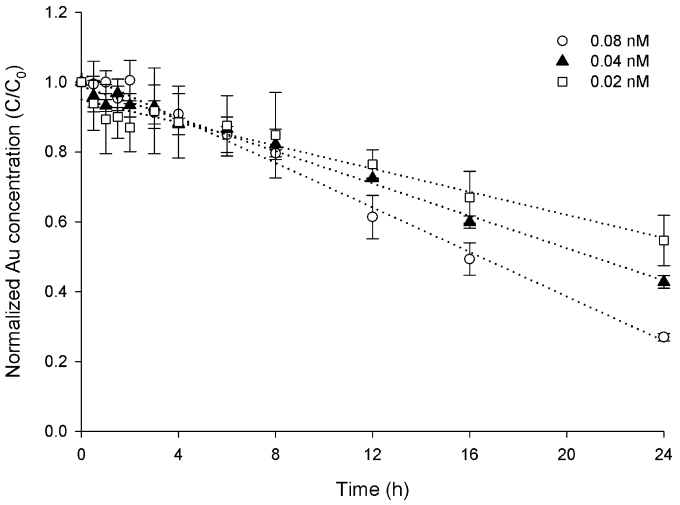

Fig. 1. Variation of total Au concentrations for 24 h at the upper layer of suspensions in hard water with three different AuNP concentrations. Dots and error bars represent the averages and standard deviations ($n = 3$). The dotted lines are the linear regression curve for each data set.

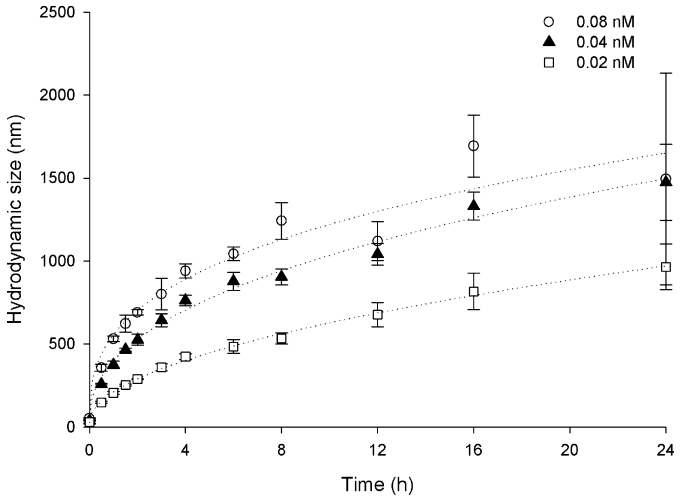

Fig. 2. The increase in hydrodynamic size (z-average) measured by DLS for suspensions of citrate-stabilized AuNPs in hard water. Dots and error bars represent the averages and standard deviations ($n = 3$). The hydrodynamic size of citrate-stabilized AuNPs was 21.64 ± 0.60 nm in DI water at 25 °C.

in both the hydrodynamic size and size by TEM indicate that AuNPs were uniform in size and well stabilized in suspension. Zeta potential is the electric potential of the NPs at the shear plane [11,24]. In terms of electrostatic stability, NPs having zeta potential less than ±20 mV are considered to be electrostatically unstable, and close approach of the particles to one another results in aggregation and settling out of suspension. Our citrate-AuNPs showed strong negative zeta potentials over the pH range of 4–10 in our stock suspension implying that AuNPs were electrostatically stable in wide range of pH due to the ionized carboxylic groups of the citrate on the AuNPs. Because zeta potentials were high enough at the pH range of 4–10 and the pHs of synthesized water used in the experiments only ranged from 7.5 to 7.9, the effect of pH on AuNP stability was negligible in the present study.

3.2. Aggregation of citrate-stabilized AuNPs in synthetic waters

The UV–vis spectrum showed that the aggregation and sedimentation of citrate-stabilized AuNPs occurred quickly in hard water (Supporting information Fig. S3). Although the UV–vis spectrum was stable over 24 h for citrate-stabilized AuNPs in DI water, a bimodal peak was immediately detected in hard water indicating that rapid initial aggregation of AuNPs occured. The peak at 521 nm in UV–vis spectrum of AuNPs in hard water, which is identical to the stable peak in deionized water, represents the monodisperse AuNPs. This absorbance decreased with time, which resulted from the loss of monodisperse AuNPs by aggregation in hard water. Another peak appeared at 680–700 nm, indicating that citrate-stabilized AuNPs formed aggregates immediately after addition to hard water. The peak at 680–700 nm broadened, red-shifted and the absorbance decreased with time indicating the growth and sedimentation of the aggregates. The decreased absorbance implied the decrease in Au concentrations in the upper layer of the suspension (Fig. 1). Au concentrations in the upper layers of suspensions decreased with time in hard water at all initial concentrations (0.02, 0.04, and 0.08 nM AuNPs). After 24 h, Au concentration decreased by 45.4 ± 7.2, 57.2 ± 1.8, and 73.1 ± 1.1% for the 0.02, 0.04, and 0.08 nM AuNPs suspensions, respectively. Dissolved Au in suspensions was not detected after filtration with 10 kDa membrane (detection limit of Au = 0.0026 μg mL^{-1}) indicating that AuNPs did not release Au^+ into hard water over the 24 h period. The sedimentation rates were −0.022, −0.058, and −0.153 mg L^{-1} h^{-1} for the 0.02, 0.04, and 0.08 nM AuNP suspensions, respectively. The results demonstrate that sedimentation rates in hard water were highly dependent on the particle concentrations.

Time-resolved dynamic light scattering experiments were employed to study the aggregate structure of AuNPs in hard water. DLS clearly showed that the hydrodynamic size of AuNPs aggregates in z-average increased with time (Fig. 2). The size determined by DLS increased from 27 nm up to >1.5 μm over 24 h. Initial rates of change in hydrodynamic size were proportional to the AuNP concentration, however after 6 h the rates were not different among three concentrations. After 24 h, the aggregates had not reached their maximum size. The fractal dimensions, D_f, of the aggregates were calculated using a simple power law relationship between hydrodynamic size and time [25–28]. The average D_f for citrate-stabilized AuNPs were 2.228 ± 0.126 (Table 2). High D_f indicated that particle-cluster aggregation occurred in hard water to form rigid structures and that the aggregation was driven by the collision of small particles to the growing aggregates due to Brownian motion [28]. Particle-cluster aggregation was indicated from UV–vis spectra. The second peak at 680–700 nm was formed very quickly and red-shifted slowly with time, implying that the aggregates grew slowly. The results suggest that once citrate-stabilized AuNPs were added to hard water, aggregates formed quickly and the single particles collided with them due to diffusion.

Generally, the growth of aggregates by single particle collision with clusters can be expressed by collision frequency of particles and collision efficiency (the ratio of aggregate formation to collisions) [29]. The time-dependent decrease in monodisperse particles, that is the aggregation rate, was expressed by first-order kinetics

$$-\frac{dN}{dt} = k_p N \quad (1)$$

where N is particle concentrations, t is time, and k_p is the aggregation rate constant which is the rate constant for disappearance of monodisperse AuNPs. Using the Lambert–Beer's law, the concentration of monodisperse AuNPs is proportional to absorbance at 521 nm. The aggregation kinetic rates were therefore determined from the UV absorbance using the expression

$$A = A_0 e^{-k_p t} \quad (2)$$

where A is UV absorbance at 521 nm at a given time, and A_0 is the UV absorbance of 521 nm at $t = 0$. Eq. (2) correlated well to the experimental data (Table 2). The aggregation rate constants ranged from

Table 2
Aggregation rate constants of citrate-stabilized AuNPs in three synthesized waters calculated by Eq. (2) and fractal dimensions in hard water at three different concentrations. Fractal dimensions were not determined for moderately hard and soft water due to the absence of hydrodynamic size data.

	Aggregation rate constant			Fractal dimension	
	C_0 (nM)	k_p (h^{-1})	r^2	D_f	r^2
Hard	0.02	0.0791 ± 0.0071	0.91 ($p < 0.01$)	2.084	1.00 ($p < 0.01$)
water	0.04	0.0794 ± 0.0071	0.93 ($p < 0.01$)	2.279	0.99 ($p < 0.01$)
	0.08	0.0836 ± 0.0040	0.98 ($p < 0.01$)	2.320	0.99 ($p < 0.01$)
Mod hard water	0.04	0.0460 ± 0.0044			
Soft water	0.04	0.0229 ± 0.0031			

0.0791 to 0.0836 h^{-1}. The aggregation rates were independent of particle concentrations and the time needed for 50% of reduction of monodisperse particles by aggregation, $t_{1/2}$, were about 8.3–8.8 h.

Citrate-stabilized AuNPs of 0.04 nM were added into moderately hard and soft waters and UV–vis and Au concentrations were measured over time. Au concentrations in the upper layer decreased for 24 h by 37.6 ± 0.8 and 33.5 ± 2.4% in moderately hard water and soft water, respectively. The rates of sedimentation determined from Au concentrations by ICP-AES were also calculated to be 0.0467 and 0.0345 mg L^{-1} h^{-1} for moderately hard water and soft water, respectively, indicating that the sedimentation was affected by the electrolyte concentration. UV–vis spectra showed results similar to those seen in the hard water experiments. Absorbance at 521 nm decreased with time and the second peak was formed immediately after addition of AuNPs in the synthetic water and red-shifted with time. Aggregation rates by Eq. (2) were proportional to the hardness as expected by the aggregation of the reaction-limited regime (Table 2).

Commonly, the stability of colloids is explained by the Derjaguin–Landau–Verwey–Overbeek (DLVO) theory which estimates that counterions can affect colloidal stability by changing the distance of closest approach for two colloids during contact [11]. Nanoparticles such as nano-sized TiO_2 have been known to readily aggregate up to micron size by increasing ionic strength with NaCl and $CaCl_2$ and the aggregation rates were highly affected by both the ionic strength and the counter ions [10] and divalent cations are reported to be far more effective for aggregation than monovalent cations [10,12]. Hardness of the synthesized water is a result of mono and divalent cations. The dependence of aggregation rate of AuNPs on hardness is explained by the fact that high ionic strength in hard water, especially the presence of divalent cations, compresses the diffuse double layer leading to the decrease in the distance between two closest particles resulting in the aggregation. The results corresponded to the fact that the aggregation of reaction-limited regime is the feature in the diluted condition like fresh water and is reported to be highly subjected to the concentration of electrolyte in suspensions [26].

3.3. AuNPs uptake by Daphnia

No mortality was seen for *D. magna* over the 48 h of exposure to 0.04 nM of AuNP. At $T = 0$, similar UV–vis spectra were observed for AuNP suspensions in both the presence and absence of *D. magna*. After 12 h, no absorbance was detected by UV–vis in the sample taken at the upper layer of suspension and Au concentration had decreased by 90.1 ± 3.5% (mean ± SD, $n = 3$)(Supporting information Fig. S4). This result did not correspond to that of previous experiment which was performed without *D. magna* and implies that *D. magna* ingested or sorbed AuNPs in hard water. After 48-h exposure to 0.04 nM of AuNPs, *D. magna* were collected and measured for Au concentration. The total Au mass in forty *D. magna* was 242.9 ± 23.2 mg (mean ± SD, $n = 3$) which corresponded to 91.2 ± 8.7% of the total Au added to the suspensions. *D. magna* was reported to be able to fill their gut within 30 min of exposure [5] and ingested nanoparticles move to the lower section of the digestive tract [30,31]. Our experiment showed a constant value for Au concentration in suspension after 12 h. This suggests that AuNPs ingested by *D. magna* reached a steady-state concentration and were not excreted back into suspension, but rather remained within the organisms. This result agreed with a previous study that showed gut fullness did not decrease for 48 h in clean media while algae feeding facilitated the depuration of particles from the digestive tract with 8 h needed for complete purging [32]. During 48-h exposure to AuNPs, *D. magna* were found to shed their external shell and these molts settled to the bottom of the containers. However in the control tests, no molts were found over the same time periods. *D. magna* are known to molt or shed their exoskeleton periodically and the newly hatched daphnia must molt several times before they are fully grown into an adult, usually after about two weeks [33]. The role of molting by *D. magna* has been reported as a means for the organism to regulate the internal concentrations of cadmium [34], mercury [35], nickel [36], and Zn [37]. Specifically, Muyssen and Janssen (2002) found that fluctuations in the total Zn in the organism occurred over 2- to 3-day intervals because about 38% of total Zn was in or on the exoskeleton which was controlled by molting. Difference in molting behavior between the AuNP exposed and the control implied an effect of AuNPs absorbed on the exoskeleton [37]. To evaluate the contribution of molts to decreasing Au body burden, molts were collected and analyzed for Au. Only 1.8% of Au (4.9 mg) was associated with molts, which is much lower than the 20–40% of Cd, Ni, and Zn that were seen in other studies to be eliminated by molting [34,36,37]. The reason *D. magna* shed their exoskeleton over the 48 h exposure to AuNPs, despite the very low amount of AuNP associated with molt, might be explained by the interference of nanoparticles on the biological behavior of *D. magna*. Nanoparticle aggregates can attach to the *D. magna* exoskeleton, appendages, and antennae [22,30]. In our study, we observed the absorption of AuNPs onto the surfaces of *D. magna* after 24 h exposure in hard water. These nanoparticles on the surface may cause the adverse effect on *D. magna* by hindering swimming or moving and in actual environmental systems may affect predation. The production of molts only in the AuNP suspensions could, therefore, be due to *D. magna* acclimation to AuNPs by removing their outer exoskeleton having sorbed nanoparticle aggregates.

We hypothesized that aggregation of AuNPs might affect the uptake or sorption of AuNPs by *D. magna*. To test the effect of aggregates, AuNP suspensions in hard water were allowed to aggregate over 48 h prior to the addition of *D. magna*. The UV–vis spectra and ICP-AES analysis confirmed aggregation of AuNPs and only 11.5% of AuNPs remained in the upper layer of suspension after 48 h. (Supporting information Fig. S5). During 48-h exposure to pre-aggregated AuNP suspension, *D. magna* survived well and produced molts and Au concentration in the upper layer did not change. This indicated that settled AuNP aggregate were not broken down and resuspended by *D. magna* movement. Similar to the previous experiment, more than 90% of AuNPs were ingested by *D. magna*. Au amounts found in molts were just 1.1% of total Au in suspensions

showing that AuNP aggregates were primarily being ingested by *D. magna* rather than absorbing onto the D. *magna* surface. Also, *D. magna* showed vigorous ingestion of AuNPs aggregates that were settled out of the suspensions. *D. magna* is a representative filter-feeding aquatic organism and are known to take up certain sizes of particles as a food through filtration of water [38]. Size exclusion mechanisms of *D. magna* make it possible to ingest particles in size range of 0.6–40 μm. Furthermore, the uptake rate had been shown to be lower for particles less than 5 μm [38]. Hydrodynamic size of monodisperse AuNPs in our experiment was about 27 nm and thus should not be filtered out by *D. magna*. The fraction of AuNPs remained in suspensions, as measured by ICP-AES, might therefore represent the monodisperse AuNPs which were not ingested due to their small size. Au concentration in molts did not show any significant difference when compared to the previous result, implying that the aggregation or size of nanoparticles did not play a role in the absorption of nanoparticles on the surface of *D. magna*.

To determine the effect of sedimentation or ionic strength on the ingestion of AuNPs, *D. magna* were exposed to AuNP suspensions in moderately hard water, which showed slower aggregation and sedimentation than in hard water (Supporting information Fig. S6). At the same AuNP concentration (0.04 nM), no mortality was found and *D. magna* molted in 48 h. *D. magna* contained 268.3 mg of Au, which corresponded to 93.8% of total Au in suspension. Only 1.4% of Au was associated with molt. The results showed that the changes of aggregation rate or sedimentation rate, due to ionic strength, did not affect the ingestion of AuNPs by *D. magna*.

4. Environmental implications of the study

Environmentally relevant conditions will likely include many other factors, such as natural organic matter and variable pH. These factors will affect the fate and transport of nanoparticles. Also nanoparticle concentration levels will be much lower than those employed in this study. Fractal dimension was independent of the particle concentrations and subject to the electrolyte concentrations in the reaction-limited regime likely to be common for freshwaters. The high fractal dimension of the study, therefore, suggests that solid or strong aggregates of AuNPs will be formed and will likely be more persistent than loose aggregates, thus making redispersion and suspension less likely. Although aggregation may limit mobility of AuNPs in the environment, it may facilitate ingestion or adhesion to aquatic organism like *D. magna*. Even though 48-h exposure to AuNPs did not show any toxic effect on *D. magna*, further study is needed to observe if chronic effects occur. It should be noted that long term exposure of *D. magna* to AuNPs may have serious toxicological effects because AuNPs are not depurated in 48 h and *D. magna* shed their exoskeleton more frequently in the AuNP suspensions as compared to the control test. Also, even if low concentrations of Au are sorbed on the molts, adhesion of nanoparticles could interfere with organism behavior and should therefore be the subject of further research.

Appendix A. Supplementary data

Supplementary data associated with this article can be found, in the online version, at doi:10.1016/j.jhazmat.2012.02.025.

References

[1] A. Neal, What can be inferred from bacterium–nanoparticle interactions about the potential consequences of environmental exposure to nanoparticles? Ecotoxicology 17 (2008) 362–371.
[2] H.E. Pace, E.K. Lesher, J.F. Ranville, Influence of stability on the acute toxicity of CdSe/ZnS nanocrystals to *Daphnia magna*, Environ. Toxicol. Chem. 29 (2010) 1338–1344.
[3] M.S. Hull, A.J. Kennedy, J.A. Steevens, A.J. Bednar, J.C.A. Weiss, P.J. Vikesland, Release of metal impurities from carbon nanomaterials influences aquatic toxicity, Environ. Sci. Technol. 43 (2009) 4169–4174.
[4] S.B. Lovern, J.R. Strickler, R. Klaper, Behavioral and physiological changes in *Daphnia magna* when exposed to nanoparticle suspensions (titanium dioxide, nano-C_{60}, and $C_{60}H_xC_{70}H_x$), Environ. Sci. Technol. 41 (2007) 4465–4470.
[5] N.A. Lewinski, H. Zhu, H.-J. Jo, D. Pham, R.R. Kamath, C.R. Ouyang, C.D. Vulpe, V.L. Colvin, R.A. Drezek, Quantification of water solubilized CdSe/ZnS quantum dots in *Daphnia magna*, Environ. Sci. Technol. 44 (2010) 1841–1846.
[6] R. Klaper, J. Crago, J. Barr, D. Arndt, K. Setyowati, J. Chen, Toxicity biomarker expression in daphnids exposed to manufactured nanoparticles: changes in toxicity with functionalization, Environ. Pollut. 157 (2009) 1152–1156.
[7] N.C. Mueller, B. Nowack, Exposure modeling of engineered nanoparticles in the environment, Environ. Sci. Technol. 42 (2008) 4447–4453.
[8] F. Gottschalk, T. Sonderer, R.W. Scholz, B. Nowack, Modeled environmental concentrations of engineered nanomaterials (TiO_2, ZnO, Ag, CNT, Fullerenes) for different regions, Environ. Sci. Technol. 43 (2009) 9216–9222.
[9] J. Fabrega, S.R. Fawcett, J.C. Renshaw, J.R. Lead, Silver nanoparticle impact on bacterial growth: effect of pH, concentration, and organic matter, Environ. Sci. Technol. 43 (2009) 7285–7290.
[10] R.A. French, A.R. Jacobson, B. Kim, S.L. Isley, R.L. Penn, P.C. Baveye, Influence of ionic strength, pH, and cation valence on aggregation kinetics of titanium dioxide nanoparticles, Environ. Sci. Technol. 43 (2009) 1354–1359.
[11] T. Laaksonen, P. Ahonen, C. Johans, K. Kontturi, Stability and electrostatics of mercaptoundecanoic acid-capped gold nanoparticles with varying counterion size, ChemPhysChem 7 (2006) 2143–2149.
[12] Y. Wang, Y. Li, K.D. Pennell, Influence of electrolyte species and concentration on the aggregation and transport of fullerene nanoparticles in quartz sands, Environ. Toxicol. Chem. 27 (2008) 1860–1867.
[13] S.D. Brown, P. Nativo, J.-A. Smith, D. Stirling, P.R. Edwards, B. Venugopal, D.J. Flint, J.A. Plumb, D. Graham, N.J. Wheate, Gold nanoparticles for the improved anticancer drug delivery of the active component of oxaliplatin, J. Am. Chem. Soc. 132 (2010) 4678–4684.
[14] X. Liu, Q. Dai, L. Austin, J. Coutts, G. Knowles, J. Zou, H. Chen, Q. Huo, A one-step homogeneous immunoassay for cancer biomarker detection using gold nanoparticle probes coupled with dynamic light scattering, J. Am. Chem. Soc. 130 (2008) 2780–2782.
[15] M.M. Maye, J. Luo, Y. Lin, M.H. Engelhard, M. Hepel, C.-J. Zhong, X-ray photoelectron spectroscopic study of the activation of molecularly-linked gold nanoparticle catalysts, Langmuir 19 (2002) 125–131.
[16] H. Hartshorn, C.J. Pursell, B.D. Chandler, Adsorption of CO on supported gold nanoparticle catalysts: a comparative study, J. Phys. Chem. C 113 (2009) 10718–10725.
[17] B.V. Enustun, J. Turkevich, Coagulation of colloidal gold, J. Am. Chem. Soc. 85 (1963) 3317–3328.
[18] J. Kimling, M. Maier, B. Okenve, V. Kotaidis, H. Ballot, A. Plech, Turkevich method for gold nanoparticle synthesis revisited, J. Phys. Chem. B 110 (2006) 15700–15707.
[19] V.L. Pallem, H.A. Stretz, M.J.M. Wells, Evaluating aggregation of gold nanoparticles and humic substances using fluorescence spectroscopy, Environ. Sci. Technol. 43 (2009) 7531–7535.
[20] US. Environmental Protection Agency, Methods for measuring the acute toxicity of effluents and receiving waters to freshwater and marine organisms, Washington DC (2002).
[21] A. Baun, N. Hartmann, K. Grieger, K. Kusk, Ecotoxicity of engineered nanoparticles to aquatic invertebrates: a brief review and recommendations for future toxicity testing, Ecotoxicology 17 (2008) 387–395.
[22] E.J. Petersen, J. Akkanen, J.V.K. Kukkonen, W.J. Weber, Biological uptake and depuration of carbon nanotubes by *Daphnia magna*, Environ. Sci. Technol. 43 (2009) 2969–2975.
[23] Z. Sun, V. Nicolosi, D. Rickard, S.D. Bergin, D. Aherne, J.N. Coleman, Quantitative evaluation of surfactant-stabilized single-walled carbon nanotubes: dispersion quality and its correlation with zeta potential, J. Phys. Chem. C 112 (2008) 10692–10699.
[24] W. Stumm, J.J. Morgan, Aquatic Chemistry: An Introduction Emphasizing Chemical Equilibria in Natural Waters, 1st ed., Wiley-Interscience, New York, 1970.
[25] S.E. Mylon, K.L. Chen, M. Elimelech, Influence of natural organic matter and ionic composition on the kinetics and structure of hematite colloid aggregation: implications to iron depletion in estuaries, Langmuir 20 (2004) 9000–9006.
[26] D. Grolimund, M. Elimelech, M. Borkovec, Aggregation and deposition kinetics of mobile colloidal particles in natural porous media, Colloids Surf. A 191 (2001) 179–188.
[27] H. Holthoff, S.U. Egelhaaf, M. Borkovec, P. Schurtenberger, H. Sticher, Coagulation rate measurements of colloidal particles by simultaneous static and dynamic light scattering, Langmuir 12 (1996) 5541–5549.
[28] G.C. Bushell, Y.D. Yan, D. Woodfield, J. Raper, R. Amal, On techniques for the measurement of the mass fractal dimension of aggregates, Adv. Colloid Interface Sci. 95 (2002) 1–50.
[29] W. Stumm, Chemistry for the Solid–Water Interface: Processes at the Mineral-water and Particle-water Interface in Natural Systems, John Wiley & Sons, Inc., New York, 1992.
[30] A. Baun, S.N. Sørensen, R.F. Rasmussen, N.B. Hartmann, C.B. Koch, Toxicity and bioaccumulation of xenobiotic organic compounds in the presence of aqueous suspensions of aggregates of nano-C60, Aquat. Toxicol. 86 (2008) 379–387.

[31] S.B. Lovern, H.A. Owen, R. Klaper, Electron microscopy of gold nanoparticle intake in the gut of *Daphnia magna*, Nanotoxicology 2 (2008) 43–48.
[32] P.L. Gillis, P. Chow-Fraser, J.F. Ranville, P.E. Ross, C.M. Wood, Daphnia need to be gut-cleared too: the effect of exposure to and ingestion of metal-contaminated sediment on the gut-clearance patterns of *D. magna*, Aquat. Toxicol. 71 (2005) 143–154.
[33] D. Martin-Creuzburg, S.A. Westerlund, K.H. Hoffmann, Ecdysteroid levels in *Daphnia magna* during a molt cycle: Determination by radioimmunoassay (RIA) and liquid chromatography-mass spectrometry (LC-MS), Gen. Comp. Endocrinol. 151 (2007) 66–71.
[34] G.C. Carney, P. Shore, H. Chandra, The uptake of cadmium from a dietary and soluble source by the crustacean daphnia magna, Environ. Res. 39 (1986) 290–298.
[35] K.E. Biesinger, L.E. Anderson, J.G. Eaton, Chronic effects of inorganic and organic mercury on *Daphnia magna*: toxicity, accumulation, and loss, Arch. Environ. Contam. Toxicol. 11 (1982) 769–774.
[36] T.M. Hall, Free ionic nickel accumulation and localization in the freshwater zooplankter, *Daphnia magna*, Limnol. Oceanogr. 27 (1982) 718–727.
[37] B.T.A. Muyssen, C.R. Janssen, Accumulation and regulation of zinc in *Daphnia magna*: links with homeostasis and toxicity, Arch. Environ. Contam. Toxicol. 43 (2002) 0492–0496.
[38] W. Geller, H. Müller, The filtration apparatus of *Cladocera*: filter mesh-sizes and their implications on food selectivity, Oecologia 49 (1981) 316–321.